

Shallow travel-time tomography below southern Mexico

Eduardo Huesca-Pérez* and Allen Husker

Received: July 25, 2011; accepted: May 03, 2012; published on line: June 29, 2012

Resumen

Se desarrollaron dos tomografías de tiempo de viaje para las ondas P y S, así como un mapa del cociente V_p/V_s en el sur de México. Se utilizaron datos provenientes de la red temporal de banda ancha Meso-American Subduction Experiment (MASE). Los perfiles de las tomografías tienen su origen en la costa del Pacífico y corren tierra adentro 205 km perpendiculares a la trinchera; muestrean hasta una profundidad de 55 km. Los resultados muestran, para ambas ondas, velocidades altas desde la costa hasta 40 km en la sección descendiente de la placa subducida de Cocos, una anomalía lenta para la onda P entre los 50 km y 90 km, por arriba del doblez donde la placa se vuelve subhorizontal y velocidades bajas para las ondas P y S por encima de la placa entre los 90 km y 205 km desde la costa. El mapa del cociente de V_p/V_s exhibe dos zonas de valores altos: (1) la región donde la placa desciende desde la costa hasta 60 km; y (2) entre los 90 km y 160 km, donde se han detectado los Tremores No-Volcánicos (NVT). Por otro lado, se encuentran valores bajos de V_p/V_s donde la placa dobla (60 km – 90 km), lo que probablemente indica que la corteza está seca y sometida a esfuerzos intensos. Se estimaron valores normales de V_p/V_s en la corteza al norte de 160 km de la costa, a pesar de que existe mucha evidencia de alta presión de fluidos en aquella región. Este hecho, muy probablemente, describe una combinación de reducciones proporcionales entre las velocidades de P y S debido a altas temperatura y bajas presiones efectivas.

Palabras clave: tomografía sísmica de tiempo de viaje, cociente de V_p/V_s , tremor no-volcánico, prueba de checkerboard.

Abstract

P and S wave travel-time tomographies as well as a V_p/V_s ratio image of the crust below southern Mexico were developed using data from the Meso-American Subduction Experiment (MASE) broad-band temporary network. The profile used in the tomography starts at the Pacific coast and runs 205 km inland perpendicular to the trench with a depth of 55 km. Results show fast P and S-wave velocities from the coast to 40 km inland in the descending section of the Cocos slab, a low P-wave anomaly between 50 km and 90 km above the corner where the slab becomes subhorizontal and low P and S-wave velocities above the slab between 90 and 205 km. The V_p/V_s image shows two areas with high values: (1) the zone where the slab descends from the coast to 60 km inland; and (2) between 90 km – 160 km from the coast where Non-Volcanic Tremors (NVT) are also found to occur. Low V_p/V_s values are found where the slab bends (60 km – 90 km) probably due to it being a highly stressed, dry region of the crust. Normal V_p/V_s values are found within the crust farther than 160 km from the coast despite strong evidence of high pore fluid pressure in that region. This is probably due to the proportional reduction of the P-wave velocity with the S-wave velocity due to high temperature and low effective pressure.

Key words: travel-time seismic tomography, V_p/V_s ratio, non-volcanic tremor, checker board test.

E. Huesca-Pérez*
Posgrado en Ciencias de la Tierra
Instituto de Geofísica
Universidad Nacional Autónoma de México
Ciudad Universitaria
Delegación Coyoacán, 04510
México D.F., México
*Corresponding autor: ehuesca@gmail.com

A. Husker
Instituto de Geofísica
Universidad Nacional Autónoma de México
Ciudad Universitaria
Delegación Coyoacán, 04510
México D.F., México

Introduction

The Mexican subduction zone has one of the few flat slab segments in the world (e. g. Gutscher *et al.*, 2000). The flat tectonic configuration of the Cocos slab below Mexico affects a wide geographic area of the overriding crust and knowledge of its geometry is important. Pérez-Campos *et al.* (2008) provided detailed seismic observations of the portion of the Cocos slab zone with the flat segment. They found in a receiver function study the subducting slab dipping at a 15° angle into the mantle, turning flat approximately 70 km from the coast at ~40 km depth. The slab remains flat until 300 km inland from the coast where it turns to steep subduction and descends into the mantle. The flat slab is mechanically decoupled from the upper crust by a very thin low viscosity zone (Song *et al.*, 2009; Kim *et al.*, 2010), probably generated by dewatering processes. It is well known that the Cocos slab is highly hydrated (Jödicke *et al.*, 2006; Manea *et al.*, 2010; Kim *et al.*, 2010) and releases its fluid content into the upper continental crust while subducting. The dehydration process makes the continental crust undergo chemical and elastic parameter changes affecting the seismic wave propagation velocities.

There is ample evidence of fluids present in the slab and the continental crust. For example, Kim *et al.* (2010) in a receiver function study find moderate to high V_p/V_s values in the upper subducted oceanic crust indicating that there exists elevated pore pressure due to fluid saturation. Iglesias *et al.* (2010) detect low shear wave velocities south of the Trans-Mexican Volcanic Belt (TMVB) over the flat section of the subducted oceanic crust that they correlate to dewatering processes from the slab. Those findings concur with a Magnetotelluric (MT) study done by Jödicke *et al.* (2006) that finds the presence of conductive anomalies that they interpret as slab-released fluids stored in the overlying continental crust. Jödicke *et al.* (2006) propose that the fluids in the MT study are thought to be progressively discharged by metamorphic dehydration of the underlying oceanic crust due to lithostatic pressure squeezing of open pores and cracks of sediments and basalts and intense “bend faulting”.

The isolated conductivity anomalies found by Jödicke *et al.* (2006) north of 105 km from the coast coincide with an area where dehydration phase changes were inferred (Manea *et al.*, 2010). This is the region where NVT energy distribution has been detected in Guerrero, Mexico within the flat slab region, 85 km to 160 km from the coast (Husker *et al.*, 2012; Kostoglodov *et al.*, 2010; Payero *et al.*, 2008). The existence of NVT could be related to the fluids released by dehydration during phase changes in the slab (Manea *et al.*, 2004; Manea *et al.*, 2010).

In this study we perform body wave tomography using P- and S-wave arrival times. Pore fluid pressure in the crust affects the velocity of seismic waves so a travel-time tomography study can provide information about the location and distribution of fluid-rich areas. The data used come from the MASE network that consisted of a 100-station seismic broadband array that was deployed during 2005 – 2007 across central Mexico (Figure 1). The array is oriented nearly perpendicular (~N16°E) to the Middle America Trench (MAT) from Acapulco on the Pacific coast to Tempoal, near the Gulf of Mexico in the north with a density of 5 – 6 km spacing between stations.

Data and Method

In order to develop the tomographic images we read the P and S wave arrival times from Mexican earthquakes registered by the MASE array. To constrain the inversion from the south, we employed the seismicity at the Mexican Pacific coast and from the north we used the seismicity of the Trans-Mexican Volcanic Belt (TMVB), the seismicity of the Valley of Mexico and one earthquake from the Gulf of Mexico (Figure 1). The Pacific seismicity comes from a catalog of Mexican earthquakes (Iglesias *et al.*, 2010) that were relocated with the double difference method (Waldhauser and Ellsworth, 2000) using the velocity model of Campillo *et al.* (1996). The Servicio Sismológico Nacional (SSN) reported 303 earthquakes in Mexico with $M \geq 4.5$ during December 2004 to April 2007. Of these events, only 90 could be relocated with an RMS < 0.5 s (Iglesias *et al.*, 2010). Only events that occurred 400 km (~4° epicentral distance, profile labeled A'A in Figure 1) from the nearest station of the MASE network were used. The majority of the events occurred at the coast, and so arrivals in the northern MASE stations were non-impulsive and could not be accurately determined.

To constrain the model using arrival times from the north, the TMVB earthquakes were employed. The TMVB seismicity comes from a catalog compiled with data from the Red Sísmica del Valle de México. The earthquakes in the area are relocated by Zenón Jiménez (unpublished catalog, personal communication) using a velocity model obtained for the region by Z. Jiménez (unpublished velocity model, personal communication). There were 32 earthquakes registered in the February 2005 to May 2007 period with M between 2.9 and 4.1. Because the low magnitude and low signal to noise ratio only ten earthquakes could be used in the inversion.

The total number of seismic rays obtained were 1951 for the P waves and 1344 for the S waves (Figure 2). The 400 km epicentral

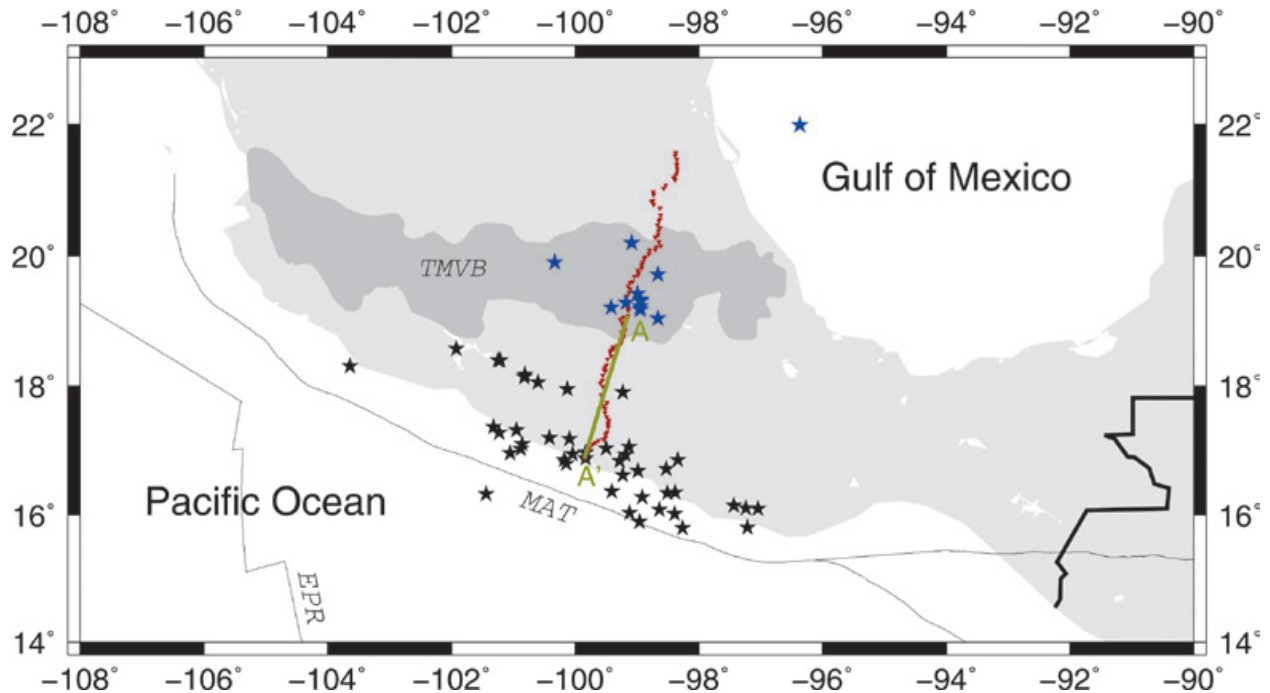


Figure 1. Map of southern Mexico showing the position of the profile of the tomography (green line labeled A'A), the MASE stations (red dots) and the seismicity used as input data (black stars, rays coming from the south; blue stars, ray coming from the north). EPR, East Pacific Rise; MAT, Middle-America Trench; TMVB, Trans-Mexican Volcanic Belt.

distance restriction limited the data set to mostly horizontal seismic rays, so multiple oblique ray-crossings that are sensitive to both vertical and lateral velocity variations could be obtained. There is good azimuthal ray coverage south of the TMVB. However seismicity is deficient to the north with just a few events between the Gulf of Mexico and the TMVB (Figure 1).

The seismograms employed were band-pass filtered between 1 and 10 Hz to remove high frequency noise and long period signals so that the time of the first arrival could be read clearly. The difference between theoretical (Campillo *et al.*, 1996) and observed arrival times, ΔT , was used as input data. Topography and the mean of the travel time were also removed from ΔT in order to account for travel time differences due to elevation and to avoid the regional offset in velocities from the Campillo *et al.* (1996) model and hypocentral errors. The topography was accounted for by assuming that regions above sea level have the same velocity as the top layer of the crustal model.

The study area consisted of a profile that runs -5 km off the coast of Acapulco, parallel to the MASE line (N16.7°E) to just south of south of Trans-Mexican Volcanic Belt (TMVB) covering a total horizontal distance of 210 km. It was not

possible to include the region north of the TMVB due to the sparse seismic activity there. The model extends to a depth of 55 km including the crust and a small part of the upper mantle. The model space was a two dimensional 15 km x 15 km grid of points and consisted of 68 grid points in all.

In order to locate station and grid spacing in kilometers instead of degrees, stations were mapped onto a flat surface using a Mercator projection with stations at the equator of the projection in order to minimize distortions in distance. The origin of the coordinate system was fixed at the Acapulco seismic station from the MASE array. A 2-D seismic ray-tracer pseudo-bending algorithm (Um and Thurber, 1987) was used to determine the ray path between the source and the receiver using the Campillo *et al.* (1996) velocity model. Because it is a shear-wave model, the corresponding P-wave vertical velocity structure was computed assuming a V_p/V_s of 1.73 (Poisson solid, i. e. the Lamé constants λ and μ are equal $V_p/V_s = \sqrt{3} \approx 1.73$). The ray tracing was performed by minimizing travel time differences by perturbing the ray path in segments (Eberhart-Phillips, 1993). In order to perform the inversion, the damped least square method (LSQR) of Paige and Saunders (1982) was used. A 2-D Gaussian filter was applied after inverting to smooth sharp shapes to get

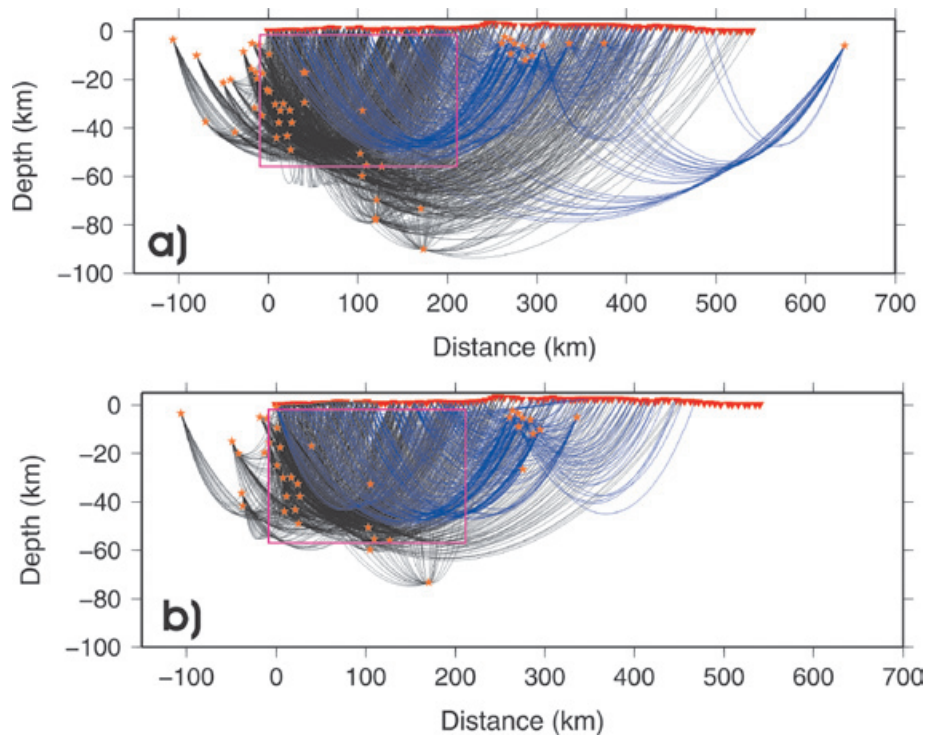


Figure 2. a) 1951 P-wave ray paths; and b) 1344 S-wave ray paths used in this study. Zero represents the first station (ACAP) of the MASE line and the origin of the tomographic profile. Black ray paths represent seismic waves coming from the south while the blue ones are coming from the north. Inverted red triangles are MASE stations; orange stars are the hypocenters. The pink rectangle shows the area encompassed by the tomographic profile.

a more robust average velocity structure. We also performed a checkerboard resolution test to ensure robustness of the results.

Results

Figures 3 and 4 show the P- and S-wave tomograms, respectively. The black continuous line represents the top of the subducted Cocos slab for comparison (Pérez-Campos *et al.*, 2008). The color scale varies from high velocity (blue) to low velocity (red). The mean velocity has been removed, so it is not possible to distinguish average velocity difference from the background model.

Figure 3 shows the P-wave tomogram where fast velocities are observed in the section of the descending slab close to the coast (blue region between 0 – 40 km). Above the corner where the slab turns horizontal there are low P-wave velocities (red-orange region between 50 km to 90 km inland). Over the flat part of the slab there is a region of slightly low velocities (red-orange region between 90 km to 160 km inland) followed by extremely low velocities to the north more than 160 km inland (red region between 160 – 205 km).

The S-wave (Figure 4) velocities exhibit some differences from the P-waves (Figure 3). In the descending slab there are fast velocities between the coast (A') to 80 km inland and 5 km to 30 km depth (blue region in Figure 4) and low velocities

more than 30 km depth (red-orange region). To the north, the tomogram shows normal velocities just above the bending section of the slab (as depicted by the green region between 80 km to 110 km inland) and almost near-normal S-wave velocities above the flat section of the slab more than 110 km inland (red-orange region).

Figure 5 shows the V_p/V_s ratio along the profile. In the image two high V_p/V_s ratio bands are formed. The first of them emerges along the dipping segment of the subducted slab (between 0 and 60 km inland) and the second between 90 and 160 km inland and both bands showing ratios greater than 1.76. Between 160 km and 205 km from the coast the V_p/V_s ratio shows almost no anomaly as depicted by the green color that corresponds to a Poisson solid. This is due to the low values in both the P- and S-wave velocities. Between 60 km and 90 km from the coast the V_p/V_s ratio shows a low anomaly with values below 1.73 just above where the slab becomes flat shown as yellow. This anomaly is due to low P-wave velocities and almost no affected S-wave velocities.

Resolution tests

We determined the resolution of the inversion using a checkerboard test (Hearn and Clayton, 1986). The checkerboard is an extreme velocity test because it has singularities at jumps between slow and fast anomalies that are not likely in nature. The resolution, in this test, of

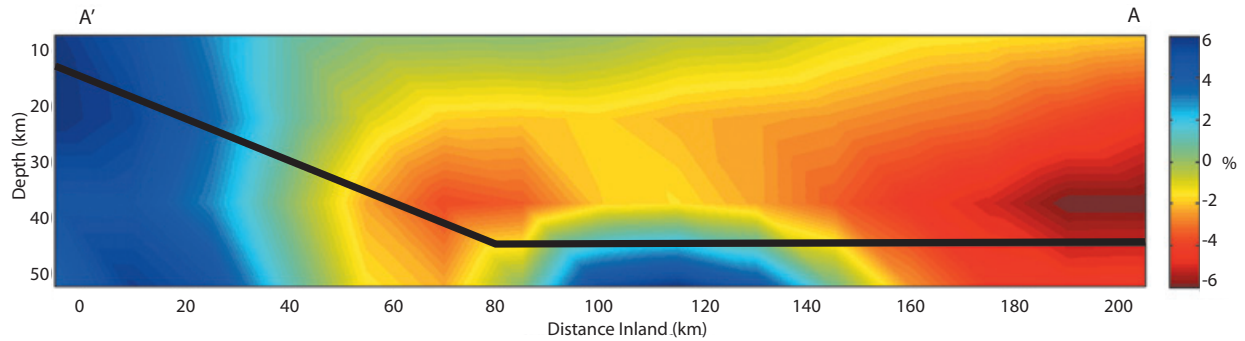


Figure 3. P wave travel time tomography. Colors represent variation of the P-wave velocity perturbation to the *Campillo et al.* (1996) background velocity model. The black continuous line represents the position of the top of the subducting Cocos slab (*Pérez-Campos et al.*, 2008). The blue and red colors represent the maximum positive and negative velocity differences from the background model, in percentage. The horizontal distance has its origin at the coast and runs inland corresponding to the profile A'A in figure 1.

a given region is found by creating a synthetic forward model of anomalies where a series of boxes are positively or negatively perturbed over and below a certain input average velocity model. The position of the original checkerboard is marked as light gray lines in Figures 6 and 7. Then, synthetic travel times are found using this synthetic structure where the ray paths are those used in the tomography. The synthetic travel times are then inverted to determine how well the synthetic velocity structure is recovered and a Gaussian filter is used to replicate the procedure used for the tomographic inversion of the real data.

The checkerboard inversions indicate that anomalies of 30 km x 30 km for the P-wave (Figure 6 panel **a**) and 50 km x 30 km for the S-wave (Figure 7 panel **b**) can be resolved in most of the profile. It is difficult to resolve smaller coherent structures as shown for the S-wave case in panel a Figure 7. Due to deficient ray coverage to the north of the profile, neither the

P-wave nor the S-wave can recover structures less than 60 km horizontal x 30 km vertical in that region (panels **c** in Figures 6 and 7). The smearing and distorted boxes amplitudes come mainly from the lack of crossing rays (sparse in the north (> 120 km) in the inversion) which is the greatest source for error in a tomographic inversion. In general more fine structures can be recovered in the southern portion of the profile due to the larger number of crossing raypaths (Figure 2). The relative strength of the velocity perturbation within the profile is reduced from 8 to 4% because of the smearing of the image (*Husker and Davies*, 2009) which gives a 4% of error in the velocity amplitude.

Discussion

In this study we obtained an image of the velocity structure as well as a map of the V_p/V_s distribution in the upper mantle, the subducted slab and crust below southern Mexico. The results show low velocity just above the slab for both

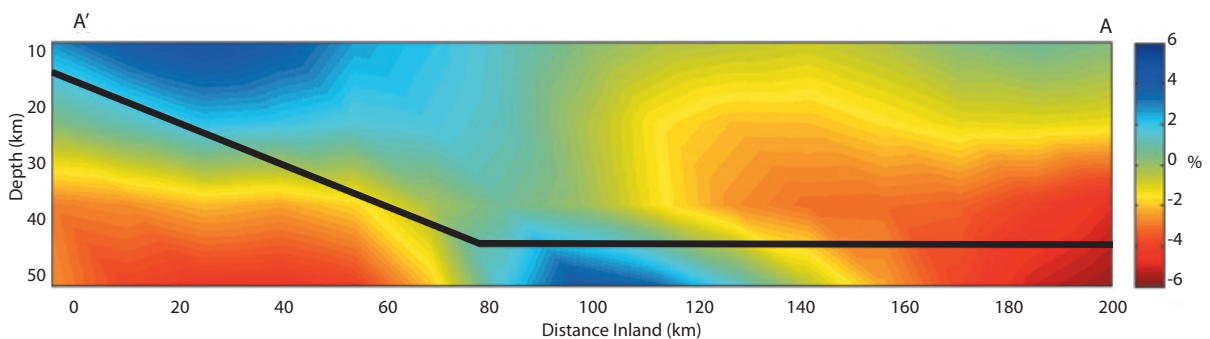


Figure 4. S wave travel time tomography. Colors represent variation of the S-wave velocity perturbation to the *Campillo et al.* (1996) background velocity model. The black continuous line represents the position of the top of the subducting Cocos slab (*Pérez-Campos et al.*, 2008). The blue and red colors represent the maximum positive and negative velocity differences from the background model, in percentage. The horizontal distance has its origin at the coast and runs inland corresponding to the profile A'A in figure 1.

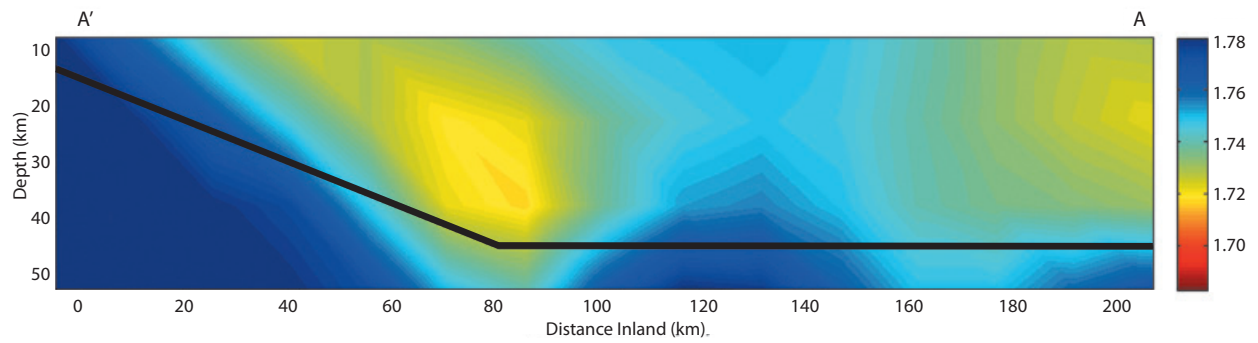


Figure 5. The color image represents the V_p/V_s ratio inversion. Green is no anomaly (Poisson solid). Blue is a high ratio whereas yellow to red are low. Black line is the position of the top of the Cocos slab (Perez-Campos *et al.*, 2008) for comparison. Label A'A refers to profile line in figure 1.

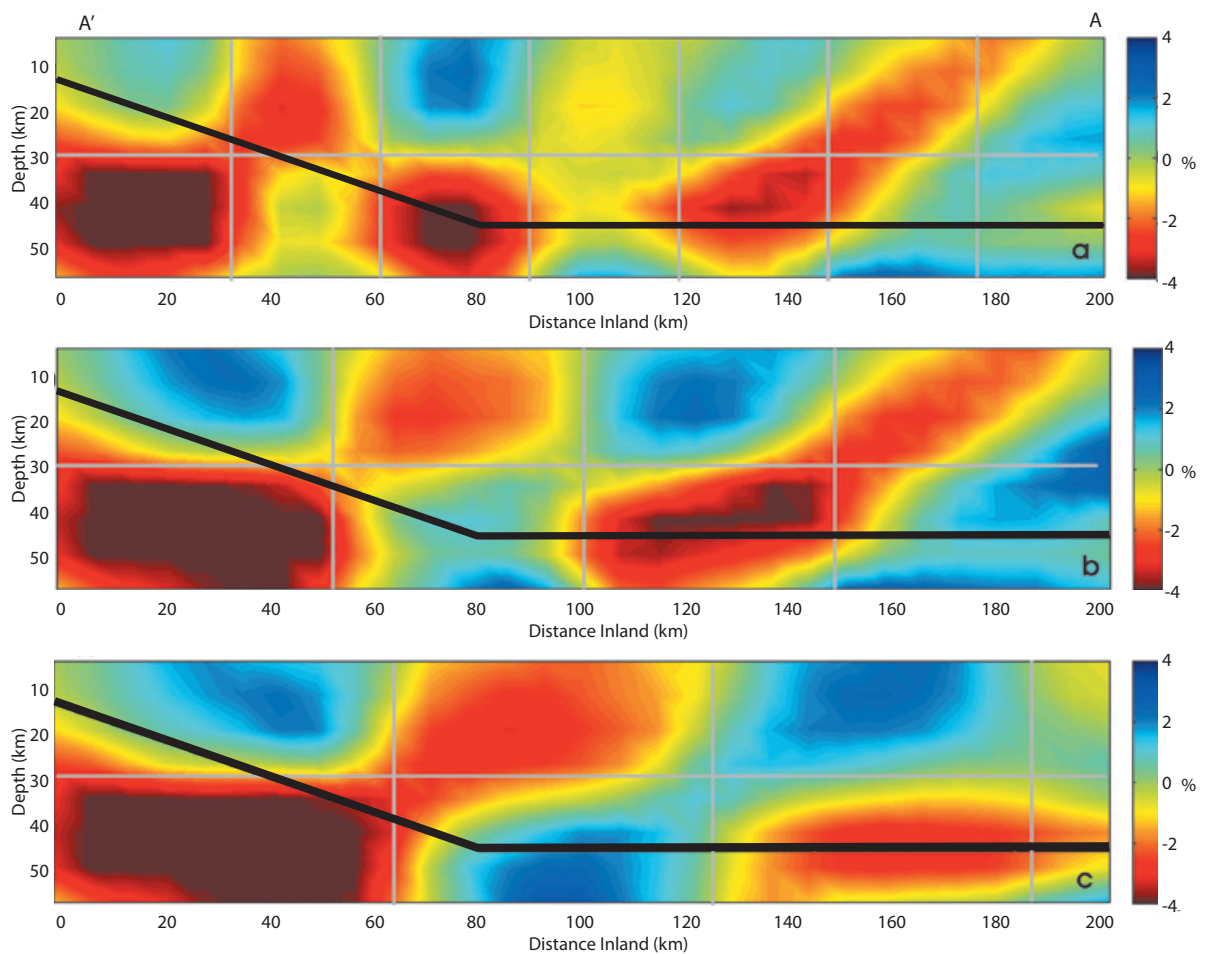


Figure 6. Checkerboard test for P-wave travel time tomography. The test consists of alternating boxes of high (blue) and low (red) velocity perturbations ($\pm 8\%$) of the background velocity model. The synthetic test is designed to show the ability of the inversion to resolve structures. Panels **a**, **b** and **c** show boxes sizes of 30 km x 30 km, 50 km x 30 km and 60 km x 30 km, respectively. Light grey lines denote the position of the original checkerboard.

waves to the north between 100 km and 205 km from the coast (A') (P and S, Figures 3 and 4). These features coincide with observations in previous studies (e. g. Jödicke *et al.*, 2006; Manea *et al.*, 2010) that suggest fluids released into the continental crust from the oceanic crust (see Figure 8, yellow area in panel d and big blue drops panels **c** – **d**). This dehydration process, represented as blue drops in Figure 8, tends to occur in several areas with different amounts of water discharge (Manea *et al.*, 2010).

There is evidence of water in the crust above nearly the entire portion of the flat slab. Manea *et al.* (2010) define two principal dewatering pulses (at 90 km – 120 km and 140 km – 180 km) associated with mineral phase changes whereas Jödicke *et al.* (2006) find a long elongated (100 km – 205 km) area of high conductivity (yellow) due to fluid presence over a larger area than reported by Manea *et al.* (2010) and confirmed here by the

tomography. The southern dewatering pulses are near a zone detected by Kim *et al.* (2010) with high Poisson's ratio in the slab that is associated with a fluid-enriched slab that releases water into the crust between 55 km – 80 km from the coast. Song *et al.* (2009) also report a fluid saturated slab and a high pore-fluid pressure zone near the coast that they interpret as trapped fluid in the down-going portion of the slab, which is released when the slab becomes flat.

Figure 5 shows the Vp/Vs ratio distribution map. Two high Vp/Vs ratio are present: (1) between the coast (A') and 60 km inland, and (2) between 90 and 160 km from the coast. The south Vp/Vs anomaly (0 – 60 km) coincides with the descending slab, which carries large amounts of water with it and where the 2006 Slow Slip Event (SSE) occurred (see also panels **c** and **d**, Figure 8). The SSE aligns with an ultra slow velocity layer (USL) found between the slab

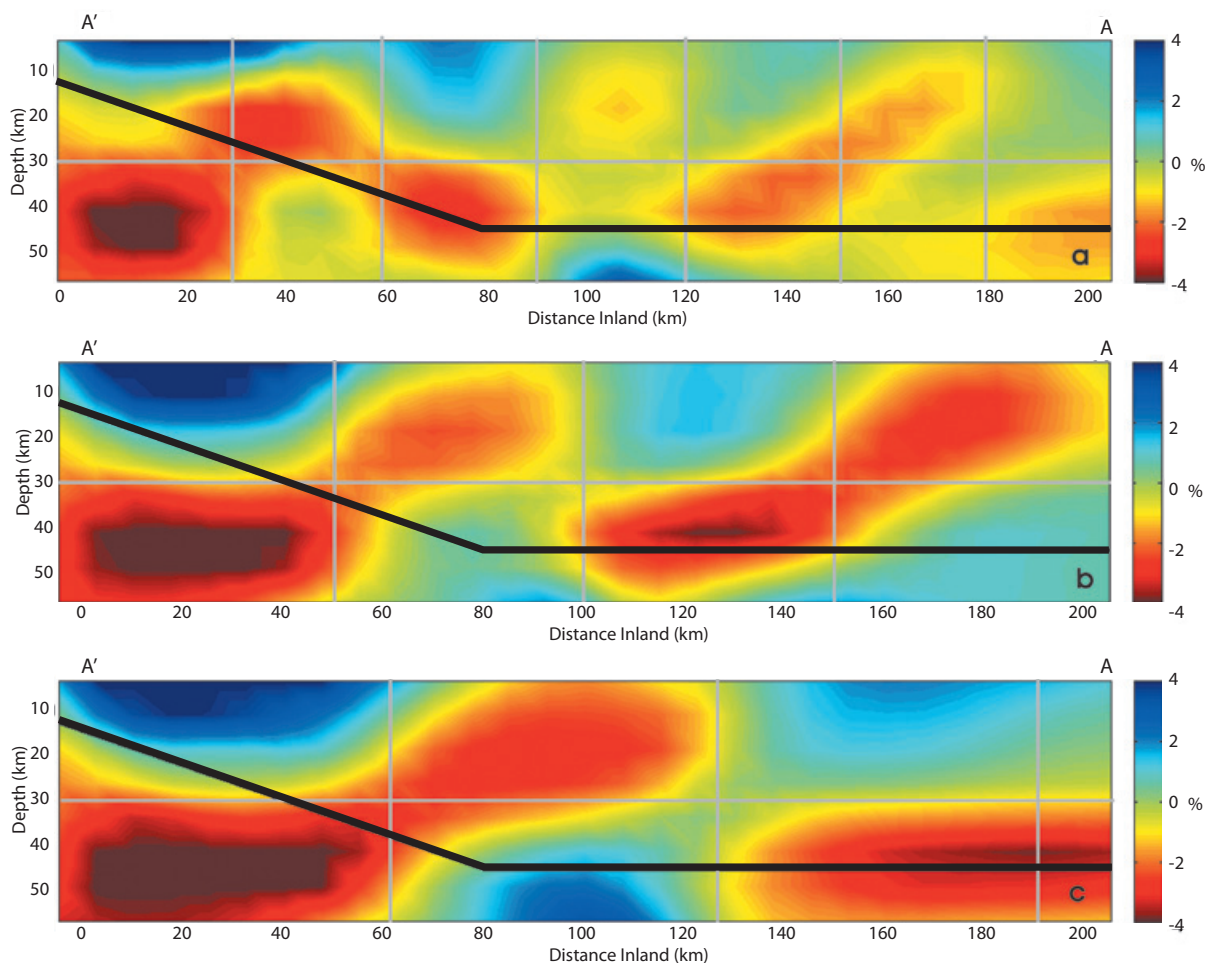


Figure 7. Checkerboard test for S-wave travel time tomography. The test consists of alternating boxes of high (blue) and low (red) velocity perturbations ($\pm 8\%$) of the background velocity model. The synthetic test is designed to show the ability of the inversion to resolve structures. Panels **a**, **b** and **c** show boxes sizes of 30 km x 30 km, 50 km x 30 km and 60 km x 30 km, respectively. Light grey lines denote the position of the original checkerboard.

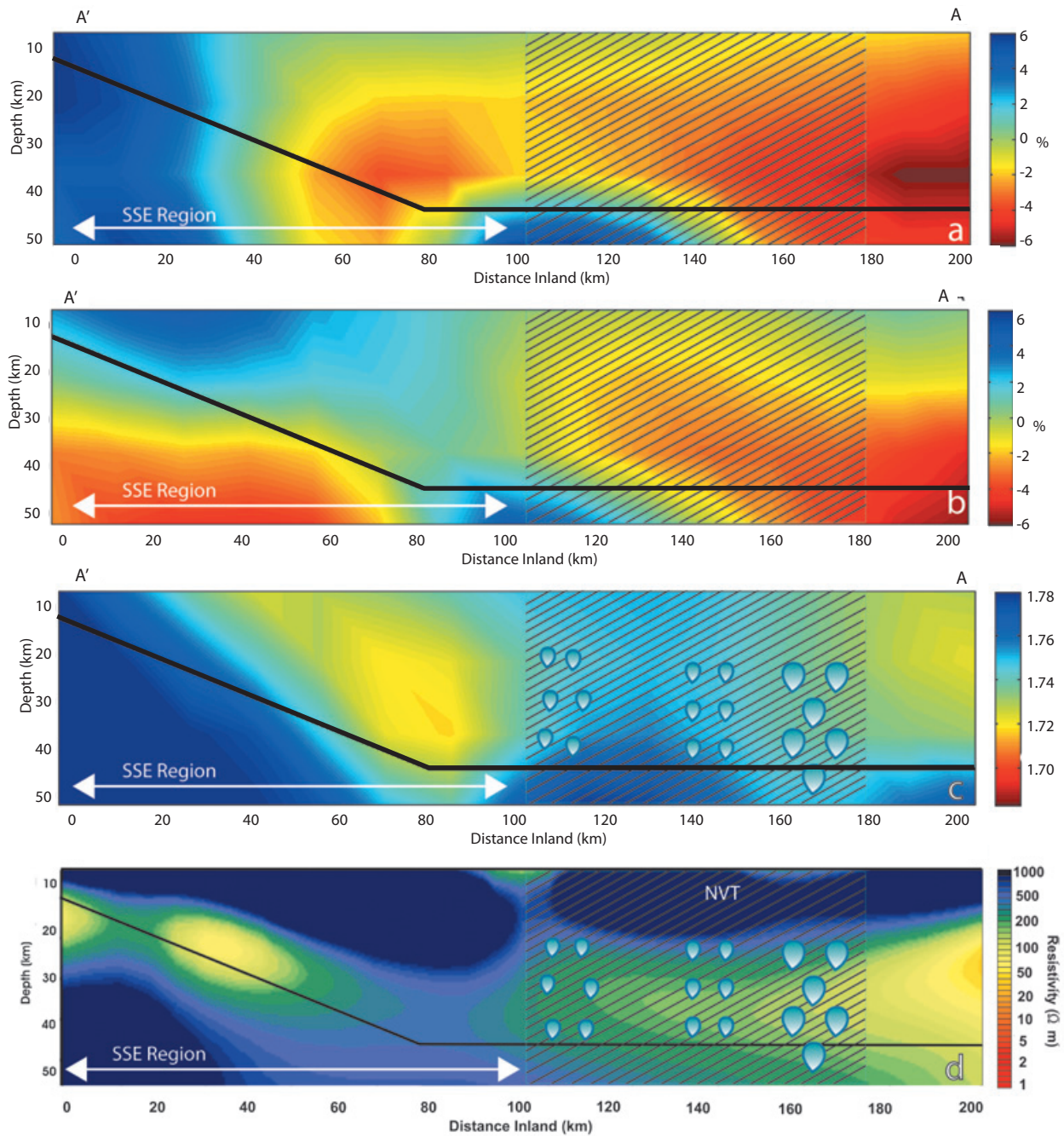


Figure 8. Interpretative comparison diagram that depicts several relevant results. The figure superimposes the tomography results (panels **a** and **b**) and the V_p/V_s ratio map (panel **c**) with the location of the NVT of *Husker et al.* (2012) delimited by the diagonal hatching and the results of *Manea et al.* (2010) where they find the presence of fluid release from the slab (blue drops panels **c** and **d**). The drops' sizes represents the quantity of liquid being released. Panel **d** shows the magnetotelluric (MT) study of *Jödicke et al.* (2006). White arrows indicate the extension of the Slow Slip Events (SSE), from the coast to 100 km inland as suggested by *Kim et al.* (2010).

and the overriding plate (Song *et al.*, 2009). USL's are evidence of high pore fluid pressure that releases partially its fluid content into the overriding crust lowering Vs and increasing the Vp/Vs ratio. Due to resolution problems it was not possible to determine the Vp/Vs ratio within USL.

The northern Vp/Vs anomaly (between 90 and 160 km, Figure 8) is high because Vs is low (Figure 8, panel **b**) indicating the presence of fluids in agreement with the other studies already mentioned. However, Vp is also somewhat low and becomes increasingly lower to the north (Figure 8, panel **a**) until Vp/Vs returns to the input value of a Poisson solid (1.73) north of 160 km (green-yellow area in Figures 5 and 8, panel **c**). The reason for the decrease in Vp is probably a combination of increased pore fluid pressure and temperature. When rock changes from dry to fluid saturated, Vs drops. However, once it is fluid saturated, Vp depends more strongly on changes in pressure and temperature than Vs (Vanorio *et al.*, 2005). Vp has been observed to decrease with decreases in differential pressure, which is lithostatic pressure minus pore pressure (Prasad and Manghnani, 1997). Horizontally within the crust, the lithostatic pressure does not change, but evidence of increased fluid content further than ~160 km from the coast (Jödicke *et al.*, 2006; Manea and Manea, 2010) suggests an increase in pore pressure, which drops the differential pressure. The simultaneous drop in differential pressure and increase in temperature with distance from the coast as inferred from Manea and Manea (2010), explains why Vp lowers with distance from the coast.

The one low Vp/Vs ratio seen as a yellow region at 80 km from the coast in Figure 5 is due to a low Vp anomaly that exists in a mostly dry media (Jödicke *et al.*, 2006; Manea and Manea, 2010) where Vs has normal values. The low Vp is probably due to a high stress regime above the bending portion of the slab where it becomes subhorizontal creating thick cracks. Thick cracks lower Vp (Shearer, 1988). The overriding crust, 40 km from the coast directly above the slab corner, seems to be in an extensive regime which is consistent with focal mechanisms of the little seismicity observed within the overriding plate (Singh and Pardo, 1993; Pérez-Campos *et al.*, 2008; Pacheco *et al.*, 2010). Singh and Pardo (1993) suggested that the extensional regime of the upper continental plate could be a consequence of trench retreat or tectonic erosion of the leading edge of the continent.

The NVT zone is located between 85 km and 160 km (Kostoglodov *et al.*, 2010; Husker *et al.*, 2012; diagonal-hatching Figure 8, panels **a** – **d**). The NVT energy bursts, in general, coincide with

a low S-wave velocity that corresponds to a high Vp/Vs ratio between 85 km – 160 km (> 1.73). The energy of the NVT bursts (diagonal-hatching, Figure 8) occurs within two fluid release pulses from the slab where temperature is near 450°C (Manea and Manea, 2010). It is unclear why the high energy NVT bursts are limited mostly to the region with high Vp/Vs. Beyond 160 km from the coast the tomography shows thermal effects of the slab hinge point, where it plunges abruptly into the mantle (Manea and Manea, 2010). The hinge point area undergoes a series of dehydration pulses between ~100 and 150 km depth (Manea and Manea, 2010) from the slab into the mantle wedge where ultramafic rocks serpentinize (Hacker *et al.*, 2003) ascending into the upper mantle and continental crust just under the active volcanoes of the TMVB. This temperature increase observed between 160 km – 205 km from the coast, induces crustal water to be super critical, increasing pore pressure and reducing Vp. The pressure and thermal conditions may indicate a limit to the presence of NVT north of 160 km from the coast.

Conclusions

Two tomography images were developed using P- and S-wave arrival times as well as a Vp/Vs ratio map below southern Mexico that sample the subducted slab and the continental crust. The tomograms show low velocity for both waves north of 100 km from the coast that suggests the presence of fluids in the crust in agreement with previous studies (e. g., Manea *et al.*, 2010; Jödicke *et al.*, 2006). A low P-wave velocity in the crust was found ~80 km from the coast just where the slab bends to become subhorizontal. A reduced S-wave velocity was not found there giving a low Vp/Vs ratio suggesting the existence of a strong stress regime that creates thick-cracks in the zone (Singh and Pardo, 1993; Pardo and Suárez, 1995; Pérez-Campos *et al.*, 2008; CMT Mexican Project). Thick cracks tend to lower Vp proportionally more than Vs (Shearer, 1988).

Two high Vp/Vs ratios are present: (1) between the coast and 70 km inland that coincides with the descending oceanic crust which carries large amounts of water where the S-wave velocity is drastically reduced and a high Poisson's ratio was detected by Kim *et al.* (2010) and where the 2006 SSE occurred; and (2) between ~100 and 160 km from the coast. Although there are evidence of fluids over almost the entire flat section of the slab (~100 to 300 km from the coast), the high Vp/Vs ratio is limited to ~100 and 160 km from the coast because of higher temperatures inferred by Manea and Manea (2010) and pore pressure north of 160 km which tend to decrease Vp. The high Vp/Vs zone (between 110 and 160 km from the coast) also corresponds to the NVT

zone (Kostoglodov *et al.*, 2010). We suggest that it is aligned to this zone due to a limit set by temperature and pressure.

Acknowledgements

We would like to thank Dr. Arturo Iglesias Mendoza for providing his seismic catalogue for Mexican earthquakes during the period 2005 – 2007 and for all his valuable advices during the development of this study. We also thank Dr Luis Quintanar Robles and the Servicio Sismológico Nacional (SSN) for providing the catalogue of the Valley of Mexico whose data has been employed in this study. Finally we thank the MASE team whose seismograms have been employed. This research was supported by CONACYT CVU 177244.

Bibliography

- Bernabei M., Botti A., Bruni F., Ricci M.A., Soper A. K., 2008, Percolation and three-dimensional structure of supercritical water, *Phys. Rev. E*, 78, 021505, 10.1103/PhysRevE.78.021505.
- Campillo M., Singh S.K., Shapiro N., Pacheco J., Hermann R.B., 1996, Crustal structure south of the Mexican volcanic belt, based on group velocity dispersion. *Geofísica Internacional*, 35, 4, 361- 370.
- Eberhart-Phillips D., 1993, Local earthquake tomography: earthquake source regions, in *Seismic Tomography: Theory and Practice*, edited by H. M. Lyer and K. Hirahara.
- Gutscher M.A., Spakman W., Bijwaard H., Engdahl E.R., 2000, Geodynamics of flat subduction: Seismicity and tomographic constraints from the Andean margin, *Tectonics*, 19, 814-833.
- Hacker B.R., Abers G.A., Peacock S.M., 2003, Subduction factory, 1, Theoretical mineralogy, densities, seismic wave speeds, and H₂O contents, *J. Geophys. Res.*, 108(B1), 2029, doi:10.1029/2001JB001127.
- Hearn Thomas M., Clayton Robert W., 1986, Lateral variations in southern California. I. Results for the upper crust from Pg waves. *Bull. Seis. Soc. Amer.* Vol. 76, No. 2. 495 – 509.
- Husker A., Davis P.M., 2009, Tomography and thermal state of the Cocos plate subduction beneath Mexico City, *J. Geophys. Res.*, 114, B04306, doi: 10.1029/2008JB006039.
- Husker A.L., Kostoglodov V., Cruz-Atienza V.M., Legrand D., Shapiro N.M., Payero J.S., Campillo M., Huesca-Pérez E., 2012, Temporal variations of non-volcanic tremor (NVT) locations in the Mexican subduction zone: Finding the NVT sweet spot, *Geochem. Geophys. Geosyst.*, 13, Q03011, doi:10.1029/2011GC003916.
- Iglesias A., Clayton R.W., Pérez-Campos X., Singh S.K., Pacheco J.F., García D., Valdés-González C., 2010, S wave velocity structure below central Mexico using high-resolution surface wave tomography, *J. Geophys. Res.* 115, no. B06307, doi 10.1029/2009JB006332.
- Jödicke H., Jording A., Ferrari L., Arzate J., Mezger K., Ruoke L., 2006, Fluid release from the subducted Cocos plate and partial melting of the crust deduced from magnetotelluric studies in southern Mexico: Implications for the generation of volcanism and subduction dynamics, *J. Geophys. Res.* 111, no. B08102, doi 10.1029/2005JB003739.
- Kim Y., Clayton R.W., Jackson J.M., 2010, Geometry and seismic properties of the subducting Cocos plate in central Mexico, *J. Geophys. Res.*, 115, B06310, doi: 10.1029/2009JB006942.
- Kostoglodov V., Husker A., Shapiro N.M., Payero J.S., Campillo M., Cotte N., Clayton R., 2010, The 2006 slow slip event and nonvolcanic tremor in the Mexican subduction zone, *Geophys. Res. Lett.*, 37, L24301, doi: 10.1029/2010GL045424.
- Manea V.C., Manea M., Kostoglodov V., Currie C.A., Sewell G., 2004, Thermal structure, coupling and metamorphism in the Mexican subduction zone beneath Guerrero. *Geophys. J. Int.* 158, 775 – 784. doi: 10.1111/j.1365-246X.2004.02325.x.
- Manea V.C, Manea M., 2010, Flat-Slab Thermal Structure and Evolution Beneath Central Mexico. *Pure Appl. Geophys.*, Springer Basel AG. Doi: 10.1007/s00024-010-0207-9.
- Pacheco J.F., Singh S.K., 2010, Seismicity and state of stress in Guerrero segment of the Mexican subduction zone, *J. Geophys. Res.*, 115, B01303, doi:10.1029/2009JB006453.
- Paige Ch. C., Saunders M.A., 1982, LSQR: An Algorithm for Sparse Linear Equations and Sparse Least Squares. *ACM Transactions on Mathematical Software*, 8, 1, 43 – 71.
- Pardo M., Suárez G., 1995, Shape of the subducted Rivera and Cocos plates in southern Mexico: Seismic and tectonic implications. *J. Geophys. Res.*, 100, 12357 – 12373.

- Payero J., Kostoglodov V., Shapiro N., Mikumo T., Iglesias A., Pérez-Campos X., Clayton R., 2008, Non-Volcanic tremor observed in the Mexican subduction zone. *Geophys. Res. Lett.* 35, L07305.
- Prasad M., Manghnani M.H., 1997, Effects of pore and differential pressure on compressional wave velocity and quality factor in Berea and Michigan sandstones, *Geophysics*, 62 (4), 1,163 - 1,176.
- Pérez-Campos X., Kim Y.H., Husker A., Davis P.M., Clayton R.W., Iglesias A., Pacheco J.F., Singh S.K., Manea V.C., Gurnis M., 2008, Horizontal subduction and truncation of the Cocos plate beneath central Mexico, *Geophys. Res. Lett.* 35, doi 10.1029/2008GL035127.
- Shearer P., 1988, Cracked media, Poisson's ratio and the structure of the upper oceanic crust. *Geoph. J.*, 92, 357 - 362.
- Singh S.K., Pardo M., 1993, Geometry of the Benioff zone and state of stress in the overriding plate in central Mexico. *Geophys. Res. Lett.*, 20, 1483 - 1486.
- Song T.R.A., Helmberger D.V., Brudzinski M.R., Clayton R.W., Davis P., Pérez-Campos X., Singh S.K., 2009, Subducting Slab Ultra-Slow Velocity Layer Coincident with Silent Earthquakes in Southern Mexico. *Science*, vol. 324, 502 - 506.
- Um J., Thurber C., 1987, A Fast Algorithm For Two-Point Seismic Ray Tracing, *Bull. Seis. Soc. Amer.*, Vol. 77, 3, 972-986.
- Vanorio T., Virieux J., Capuano P., Russo G., 2005, Three-dimensional seismic tomography from P wave and S wave microearthquake travel times and rock physics characterization of the Campi Flegrei Caldera, *J. Geophys. Res.*, 110, B03201, doi: 10.1029/2004JB003102.
- Waldhauser F., Ellsworth W.L., 2000, A double-difference earthquake location algorithm: Method and application to the northern Hayward fault, *Bull. Seism. Soc. Amer.*, 90, 1,353-1,368.